ORIGINAL ARTICLE

Effects of cambial age and flow path-length on vessel characteristics in birch

Xiping Zhao

Abstract The distribution of vessels in broadleaf timber, is directly related to water transport efficiency and safety. Here, I tested the hypothesis that vessel characteristics depend on cambial age (CA) and flow path-length (PL) within the tree rather than solely on CA by measuring vessel hydraulic diameter (VD), vessel frequency (VF), theoretical specific hydraulic conductivity (k_s), and theoretical implosion resistance (VIR) in every growth ring of birch (*Betula platyphylla* Roth.) tree root, trunk, and branch samples. The effects of CA and PL were analyzed using a linear mixed model. Differences in the vessel characteristics are significant between CA, between PL, and between the interaction of CA and PL. VD decreased linearly and VF increased nonlinearly with PL. The PL explained 59.3 and 67.3 % of the longitudinal variation in VD and VF, respectively. k_s decreased nonlinearly and VIR increased linearly with PL. The PL explained 25.6 and 43.3 % of the longitudinal variation in k_s and VIR, respectively. Radial changes were evident above ground, VD increased, and VF decreased with CA for the first 10–20 years and remained constant thereafter. k_s exhibited a logarithmic increase and VIR exhibited logarithmic decrease with CA. Variable radial patterns were observed below ground. The CA explained 30.9–98.8 %, 23.7–96.9 %, 42.9–96.8 %, and 50.9–98.5 % of the radial variation in VD, VF, k_s, and VIR, respectively. The results suggest that vessel characteristic changes are determined by CA and PL. While growing, trees adjust their vessels to maximize water transport efficiency and ensure mechanical safety.

X. Zhao (✉)
Forestry College, Henan University of Science and Technology, Luoyang 471003, Henan, China
e-mail: zhaoxiping1977@126.com

Introduction

Conduit size and frequency within a tree are spatially heterogeneous (Gartner 1995; Schulte 2012) and have important functional consequences in long-distance water transport and embolism vulnerability (Tyree and Sperry 1989; Hacke and Sperry 2001; Sperry et al. 2006; Jacobsen et al. 2007). Vessels are special conduits for water transport in hardwood xylem that vary along the flow path-length (PL) within the tree. Many researchers have found that vessel diameter decreases and frequency increases from the roots to the stem, branch, and even leaves (Leitch 2001; James et al. 2003; Fan et al. 2009; Lintunen and Kalliokoski 2010; Zach et al. 2010; Olson and Rosell 2013). The convergent pattern of conduits towards the stem apex is usually called conduit tapering (West et al. 1999; Anfodillo et al. 2006; Petit et al. 2007). It has been suggested that water is sucked up by tree roots from the soil and transported through the stem and branches to the leaf, a process that overcomes huge path-length resistance and gravity (He et al. 2007).

To maximize hydraulic conductivity and minimize xylem vulnerability, the tree should adjust its wood anatomy (e.g., by changing vessel size and number) to achieve optimal hydraulic architecture. Auxin is the determinant of wood anatomy (Aloni 1987; Plomion et al. 2001; Nilsson et al. 2008; Aloni 2013). Auxin is produced from young leaves and flows through the vascular cambium (Sundberg et al. 2000). Auxin concentration depends on the distance from the source of auxin production (the young leaves) and

decrease from the leaves to the roots (Lovisolo et al. 2002). The decreased auxin concentration resulted in a long expansion phase of slowed differentiation and, therefore, fewer and larger vessels (Czkowski 1973; Aloni 1987; Anfodillo et al. 2012).

In addition to the auxin concentration being controlled by PL, cambium age (CA) is one of the internal factors determining wood anatomy (Zobel and Buijtenen 1989; Plomion et al. 2001; Rossi et al. 2008). Xylem cells are produced by divisions in cambial initials. The cambium becomes mature, resulting in a change in the dimensions of cambial initials over time, which in turn affects the dimensions of xylem cells produced by the cambium (Plomion et al. 2001). The comprehensive radial variation of cells has been extensively studied, and the CA can fully explain the radial variation of xylem structure (Helińska-Raczkowska 1994; Rao et al. 2002; Shi et al. 2008). However, most of these measures were performed at a single stem height, i.e., breast height. There are relatively few data available on radial variation in wood anatomy at different PL (Fan et al. 2009; Lachenbruch et al. 2011).

In fact, CA and PL are closely associated. On the one hand, CA, which varies with PL within a tree, is consistent with the age of the trees in the borders of the roots and trunks and gradually decreases with increasing PL. On the other hand, the flow PL increased with decreasing CA at a certain position, which caused increased auxin concentration at the position (Lovisolo et al. 2002). All these studies showed that vessel properties vary systematically with CA and PL. However, details about within-tree vessel variations are still lacking (Bhat and Karkkainen 1981; Sellin et al. 2008).

Here, I tested the hypothesis that vessel characteristics depend on CA and PL rather than solely on CA in birch (*Betula platyphylla* Roth.) trees grown in secondary forest stands. The vessel characteristics were measured in every growth ring on samples excised from the roots, trunk, and branches. A linear mixed model was used to estimate the effects of PL and CA, as well as their interaction. Theoretical specific conductivity (k_s) and vessel implosion resistance (VIR) in different parts were calculated to better understand the effect of vessel characteristics on water transport efficiency and safety.

Materials and methods

Study material

Sampling was performed at the Maoershan Forest Ecosystem Research Station in Heilongjiang Province, northeastern China (127°30′–34′E, 45°20′–25′N, elevation 300 m). The site has an average northwest slope of 20–25°.

Table 1 Characteristics of the 10 sampled trees

Tree	Age (a)	DBH (cm)	Heigh (m)	Crown base (m)	Crown width (m)
B1	52	26.3	21.2	9	4.7
B2	55	24.4	18.4	9.1	6.4
B3	56	30	21	8.7	8.7
B4	54	23.3	18.3	10.2	6.1
B5	57	23.9	19.5	7.1	6.6
B6	53	20.7	20.2	8.4	5.6
B7	56	29.9	18.6	8.4	6.8
B8	56	23.6	20.2	7.5	7.1
B9	56	27.4	23	7	7.4
B10	56	28.5	21.7	9.3	7.2

Height and *DBH* represent tree height and diameter at breast height position, respectively. *Crown base* is the measurement of the height to the base of the live crown, while the *crown width* was estimated from the average crown radius

The parent material is a granite bedrock, while the soil is dark brown with abundant organic matter and high fertility. The climate is of continental monsoon type with the following mean annual values: 700 mm of precipitation, 884 mm of evaporation, a 2.8 °C air temperature, and a 130-day frost-free period (Wang 2006). The primary forest was dominated by Korean pine mixed with some deciduous species. After large-scale industrial logging as well as subsequent burning and destruction at the turn of the twentieth century, the current forests are mainly composed of secondary forest types (mainly *B. platyphylla*, mixed *Quercus mongolicoa*, *Populus ussuriensis*, and *Fraxinus mandshurica*).

Ten dominant trees selected for measurements of vessel characteristics were cut in August 2010 and the age of each tree was determined by the counting of its annual rings. The characteristics of the sample trees are summarized in Table 1. The crown of each tree was cut into three sections. One standard primary (I order) branch was chosen from the upper, middle, and lower canopy of each sample tree. The height and branching angles (a_1) of the I order branch were measured (Fig. 1). From each I order branch, one standard II order branch was chosen and measured for its angle (a_2) and distance from the I order branch base (l_1). From the II order branch, one standard III order branch was subsequently selected and measured for its distance from the II order branch base (l_2). For each sample tree, 3–4 horizontally oriented proximal woody roots near the soil surface were excavated using hand tools. Proximal roots are non-adventitious and directly attached to root collars (Kalliokoski et al. 2008).

Five-centimeter-thick disc samples were taken from the water transport pathway (Fig. 1). From the stem, a disc was cut at stump height (0.1 m), breast height (1.3 m), and at
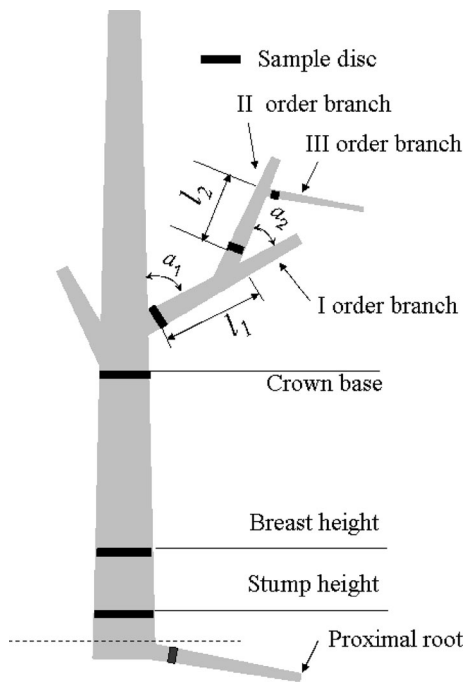
Fig. 1 Schematic of the applied sampling procedure. The disc samples and sampling locations from the water transport pathway are marked with the *black belts*. I separates the upper, middle, and lower canopies of the sampling branches. Only one I order branch and its II and III order branches are shown

the base of the live crown. From the branch or root, a disc was cut just above the basal swelling. The sampling location of the root was considered a starting point for the flow PL calculations. The PL from the root to the collection position for each of the wood discs was determined trigonometrically from the vertical height of the collection point and the horizontal distance from the base of the tree (James et al. 2003).

For the stem and I order branch samples, the height of the sampling location was considered the flow PL. For the II and III order branch samples, the flow PL could be calculated by the distance (l_1, l_2), branching angles (a_1, a_2), and the corresponding I order branch height (Figure 1). All discs were taken to the laboratory for xylem anatomy measurements.

Xylem anatomy measurements

From each collected disc, one radial strip (1 cm wide) running from the pith to the bark was randomly selected and softened by soaking in a solution of 5 % ethylenediamine. A 15-m-thick transverse section was made from each wood strip using a Leica slicing machine and then stained with 1 % safranin in water (Lin 1993). Digital images of the sections were taken using an Mshot-MD50 (Micro-shot Technology, Guangzhou, China), an easy-to-

operate digital microscope. Wood anatomical characteristics were measured ring by ring with a color image computer analysis system (TDY-5.2) as previously described (Yu et al. 2008). An average of 60 vessels were measured per tree ring.

For each individual vessel, the tangential and radial axes were determined (a_i and b_i, respectively). The vessel lumen diameter (d_i, m) was calculated as the geometric mean of the two orthogonal axes using Eq. 1:

$$d_i = \sqrt{a_i b_i} \tag{1}$$

Hydraulically weighted average vessel diameter (VD, m) were calculated using Eq. 2 (Tyree and Zimmermann 2002):

$$VD = \sqrt[4]{\frac{1}{n}\sum_{i=1}^{n} d_i^4} \tag{2}$$

The vessel frequency (VF, mm^{-2}) was calculated using the total number of vessels in an observed image area dividing by that area.

The theoretical specific hydraulic conductivity (k_s, kg m^{-1} MPa^{-1} s^{-1}) of the wood per tree ring was calculated using Eq. 3 (James et al. 2003):

$$k_s = \frac{\pi\rho}{128\eta A}\sum_{i}^{n} d_i^4, \tag{3}$$

where A (m^2) is the total area of the image fields per ring, ρ (kg m^{-3}) is the density of water at 27 °C, η (MPa s) is the dynamic viscosity of water, d_i is the diameter of single vessels, and n is the number of vessels in the total image fields.

The theoretical vessel implosion resistance (VIR) was calculated using Eq. 4 (Hacke et al. 2001):

$$VIR = \left(\frac{t}{b}\right)^2_h, \tag{4}$$

where t refers to the combined wall thickness of the adjoining vessels and b refers to the side of a square with an area equal to the average lumen diameter of the vessels.

In trees, water is transported through vessels under negative pressure. Vessels must withstand both the mechanical stresses associated with negative pressure and the risk of air entering the vessels. The strong relationship between VIR and cavitation resistance have been widely reported among diverse species (Tyree and Sperry 1989; Hacke and Sperry 2001; Sperry et al. 2006; Jacobsen et al. 2007). VIR has been accepted as the measure of vulnerability to cavitation (Martínez-Cabrera et al. 2009). The VIR was determined for those vessels within the sampled vessels per tree ring that formed pairs from which one or both vessels fell within ±5 μm of the calculated hydraulic diameter in this research.

Statistical analysis

Effects of CA and flow PL on the response variables were examined using a linear mixed model (Goldstein 2011). The hierarchical effects of the individual tree (TR) and tree compartment (TC) were accounted for using two nested levels, the TC effect being nested within the TR effect as follows:

$$Y_{ijkl} = \mu + \beta_1 CA_i + \beta_2 PL_j + \beta_3 (CA \times PL)_{ij} + \sum \beta_k TR_k \\ + \sum \beta_{(l)k} TC_{(l)k} + e_{ijkl}$$

(5)

where μ is the overall mean; CA_i, PL_j, and $(CA \times PL)_{ij}$ are the fixed effects associated with the ith CA, jth flow PL, and their interactions, respectively; TR_k and $TC_{(l)k}$ are the random effects associated with the kth tree and the lth compartment in the kth tree; e_{ijkl} is an error term; $\beta_1 - \beta_3$ are the fixed-effect coefficients; β_k and $\beta_{(l)k}$ are the random effect coefficients. The random effects TR_k and $TC_{(l)k}$ are assumed to be normally distributed with zero mean and corresponding variances σ_k^2 and $\sigma_{(l)k}^2$, whereas the error term e_{ijkl} has zero mean.

Before fitting the mixed models, scatter correction for variables were performed through standard normal variate transformation. The mixed models were fit with a restricted maximum likelihood method. The homogeneity and normality of the residuals were checked to ensure that the assumptions were met. The statistical significance ($P = 0.05$) of the fixed effects were determined using the F test. The variance components of the random effects and their standard errors were expressed as a percentage of the total variation of all of the random effects (Goldstein 2011).

The spatial variation was determined using the linear mixed model for all of the available data. The change of vessel characteristics against CA and PL was described using a linear or nonlinear model, respectively. The change of VF, k_s, and VIR against VD was described as a power (or linear) model. All of the statistical analyses were performed using SPSS software v.13.0.

Results

The mean values and standard deviations of vessel characteristics are shown in Table 2. Among-tree variation

Table 2 Descriptive statistics (mean value ± standard deviation) of geometric mean diameter (d_i), hydraulically weighted average vessel diameters (VD), vessel frequency (VF), theoretical specific hydraulic conductivity (k_s) and theoretical vessel implosion resistance (VIR)

Tree	d_i (μm)	VD (μm)	VF (mm^{-2})	k_s (kg m^{-1} MPa^{-1} s^{-1})	VIR
All samples	98.5 ± 28.3	100.9 ± 33.6	32.3 ± 10.5	217.7 ± 76.2	0.019 ± 0.006
Root	127.7 ± 13.2	133.1 ± 26.2	20.5 ± 2.7	275.1 ± 72.2	0.013 ± 0.005
Stump	125.3 ± 17.8	130.6 ± 25.9	19.5 ± 3.1	217.5 ± 75.3	0.014 ± 0.005
Breast	125.0 ± 23.0	132.9 ± 33	21.6 ± 4.6	272.0 ± 93.5	0.014 ± 0.004
Crown base	101.6 ± 20.2	107.5 ± 25.9	27.9 ± 4.3	273.1 ± 101.2	0.018 ± 0.004
I Order branch	63.8 ± 14.8	67.6 ± 18.2	43.0 ± 10.1	194.3 ± 68.0	0.027 ± 0.006
II Order branch	45.0 ± 8.4	47.4 ± 12.7	56.7 ± 6.7	141.9 ± 34.5	0.026 ± 0.003
III Order branch	35.7 ± 7.4	38.1 ± 12.2	66.7 ± 8.0	118.4 ± 28.6	0.030 ± 0.005

Table 3 Linear mixed model analysis of variance: F value for the fixed effects and variance components estimates for the random effects

Effect factors	Dependent variables			
	VD	VF	k_s	VIR
Fixed effects (F values)				
CA	333.5**	89.9**	149.7**	40.2**
PL	8.6**	111.6**	27.2**	81.4**
CA × PL	22.3**	440.0**	217.5**	164.1**
Random effects (variance components estimate ± SE %)				
TR	9.2 ± 4.2	12.8 ± 11.6	9.0 ± 1.3	12.6 ± 7.8
TC nested within TR	63.3 ± 25.8	77.9 ± 12.7	47.7 ± 13.8	42.2 ± 25.3
Residuals	27.6 ± 2.3	9.3 ± 0.7	43.7 ± 19.6	45.1 ± 0.8

The F value is the ratio of the between-group variation to the variation within group (residual or unexplained variance)

VD hydraulically weighted average vessel diameters, VF vessel frequency, k_s theoretical specific hydraulic conductivity, VIR theoretical vessel implosion resistance

** $P < 0.01$

accounted for <13 % of the total random variation in vessel characteristics (Table 3). The low among-tree variability in vessel characteristics is not surprising because the sample trees were dominant and cut from the same site. Vessel characteristics changed with flow path-length (PL) at the whole-tree level (Table 2). Among-compartment variation explained 42.2–77.9 % of the total random variation (Table 3). Compared with theoretical specific hydraulic conductivity (k_s) and theoretical vessel implosion resistance (VIR), vessel hydraulic diameters (VD) and vessel frequency (VF) showed greater variance (Table 3).

Effects of flow path-length

Along with flow path, VD decreased linearly with PL (Fig. 2a). VF had an opposite but nonlinear pattern (Fig. 2b). The PL explained 59.3 and 67.3 % of the longitudinal variation in VD and VF, respectively. Analysis of variance confirmed that the effect of PL on VD and VF was significant (Table 3), and the effect of the interaction between PL and CA was highly significant. Linear mixed model provided a good fit for VD and VF by including the
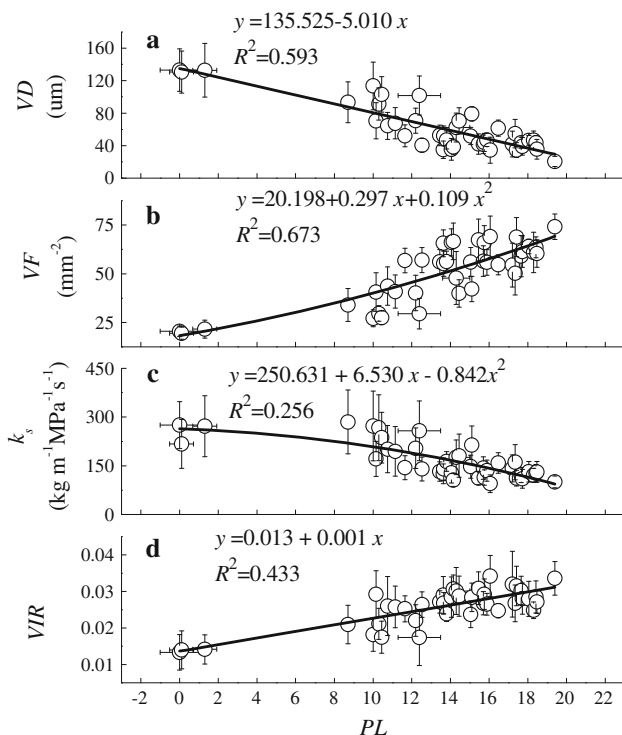
interactions and explained 66.9 and 69.9 % of their spatial variation, respectively (Table 4).

The effect of PL on k_s and VIR is significant (Table 3), while k_s exhibited a nonlinear decrease and VIR exhibited a linear increase with PL (Fig. 2c, d). The PL explained 25.6 and 43.3 % of the longitudinal variation in k_s and VIR, respectively. By including the effect of CA, PL, and their interactions, the linear mixed model explained 40.8 and 48.1 % of the spatial variation in k_s and VIR, respectively (Table 4).

Effects of cambial age

The effect of CA on VD and VF is significant (Table 3). The radial variation pattern of the vessel characteristics and hydraulic properties of the root xylem was different from those of the stem and branch. In the roots, from the pith outward, VD and VF appeared to be constant with CA (Fig. 3a, d), k_s decreased slightly during the first 40 years and then increased (Fig. 3g), and VIR increased slightly (Fig. 3j). Poor fits derived from the comparison of above-ground data with belowground data based on Table 5. The CA explained <51 % of the radial variation in vessel characteristics and hydraulic properties of the roots.

Above ground, three parts of the stems and the three orders of branches exhibited an almost uniform nonlinear increase of VD and decrease of VF with CA (Fig. 3b, c, e, f). From the pith outward, VD increased and VF decreased during the first 10–20 years and then remained constant. Logarithmic regression showed better fit. The CA explained 87.6–98.8 and 86.1–96.9 % of the radial variations in VD and VF, respectively (Table 5). However, close examination of the data showed differences in radial change rates with PL. With PL increased, the average radial change rate increased for VD and decreased for VF (Fig. 3b, c, e, f). For VD, the greatest increase rate was shown at I order branch at about two times faster

Fig. 2 Variations in hydraulically weighted average vessel diameters (VD, μm), vessel frequency (VF, mm^{-2}), theoretical specific hydraulic conductivity (k_s, kg m^{-1} MPa^{-1} s^{-1}), and theoretical vessel implosion resistance (VIR) with flow path-length (PL, m) in the sampled trees. Each data point is the mean value ± stand deviation of 10 trees. The *curves* were fitted using linear or nonlinear models shown in the figure

Plot a: $y = 135.525 - 5.010\,x$, $R^2 = 0.593$

Plot b: $y = 20.198 + 0.297\,x + 0.109\,x^2$, $R^2 = 0.673$

Plot c: $y = 250.631 + 6.530\,x - 0.842x^2$, $R^2 = 0.256$

Plot d: $y = 0.013 + 0.001\,x$, $R^2 = 0.433$

Table 4 Regression analysis of hydraulically weighted average vessel diameters (VD, μm), vessel frequency (VF, mm^{-2}), theoretical specific hydraulic conductivity (k_s, kg m^{-1} MPa^{-1} s^{-1}) and theoretical vessel implosion resistance (VIR) against cambial age (CA, a), flow path-length (PL, m), and CA × PL using the linear mixed model $y = \mu' + \beta_1 CA + \beta_2 PL + \beta_3 (CA \times PL)$

	μ'	β_1	β_2	β_3	R^2
VD	117.198	0.741	−5.128	0.067	0.669
VF	20.830	−0.067	2.406	−0.045	0.699
k_s	227.617	1.234	−10.346	0.451	0.408
VIR	0.015	−3.9E−005	0.001	−2.1E−005	0.481

Symbols β_1, β_2, β_3, and μ' are parameters of the model

R^2 is the percentage of variation explained by the model
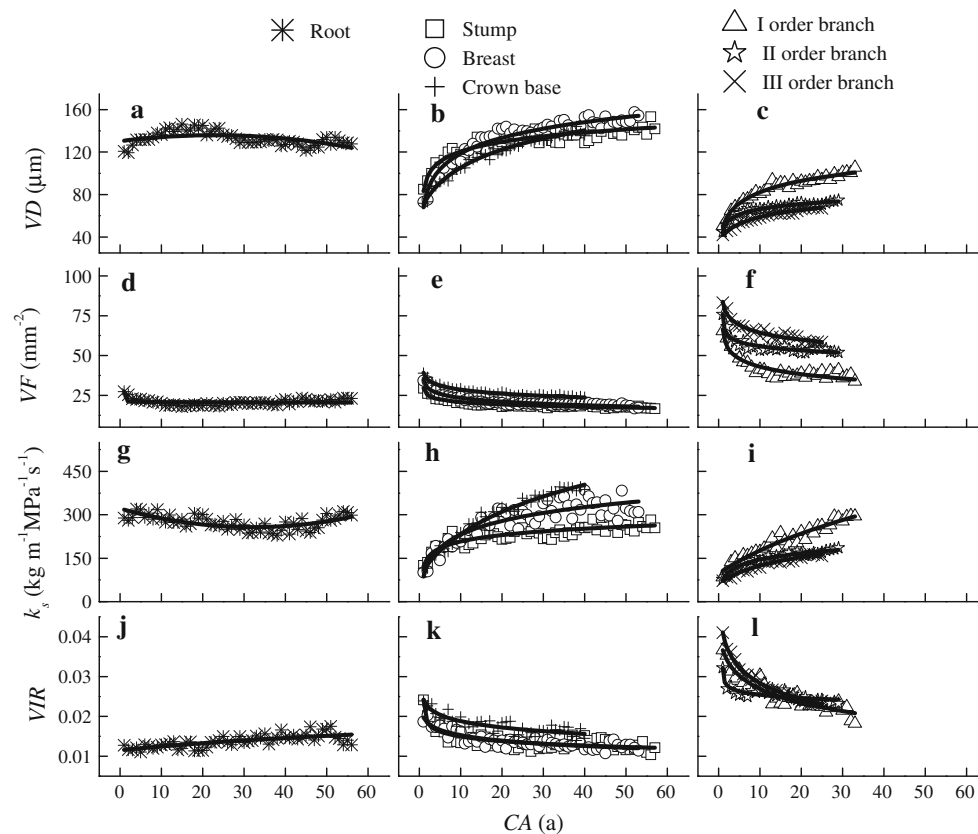
The models are all significant with $P < 0.001$

Fig. 3 Variations in hydraulically weighted average vessel diameters (*VD*, μm), vessel frequency (*VF*, mm^{-2}), theoretical specific hydraulic conductivity (*k_s*, kg m^{-1} MPa^{-1} s^{-1}), and theoretical vessel implosion resistance (*VIR*) with cambial age (*CA*, a) at different compartments in the sampled trees. Each data point represents the mean value obtained from 10 trees. The *curves* were fitted using linear or nonlinear regression functions. All of the regression models are shown in Table 5

(1.9 m year^{-1}) than at the stump (1.0 m year^{-1}). For VF, the greatest decrease rate was shown at III order branch at about two times faster (1.0 mm^{-2} year^{-1}) than at the stump (0.2 mm^{-2} year^{-1}).

In stems and branches, k_s exhibited a logarithmic increase with CA and was similar to that of VD (Fig. 3h, i). VIR exhibited a logarithmic decrease and was similar to that of VF (Fig. 3k, l). The linear mixed model revealed that k_s and VIR continued to vary significantly with CA (Table 3). The CA explained 74.5–96.8 and 69.3–98.5 % of the radial variations in k_s and VIR, respectively (Table 5).

Relationship between VF, k_s, and VIR with VD

Pooling data across all sampled trees, VF and VIR were nonlinearly decreased with VD (Fig. 4a, c). The power regressions of VF and VIR against VD explained 90.4 % of the variations in VF and 71.8 % of the variations in VIR. However, k_s was linearly increased with VD and the linear regressions explained 94.2 % of the variations in k_s (Fig. 4b).

Discussion

Effects of flow path-length

I studied the hydraulically weighted average vessel diameters (VD) and vessel frequency (VF) values in the different tree compartments of *B. platyphylla* to assess the effect of CA and PL on vessel characteristics. The differences in vessel characteristics among tree compartments (TC) are large. TC as a variable explained 63.3 and 77.9 % of the total random variations in VD and VF, respectively (Table 3). A significant difference in vessel characteristics among TC has also been observed in other studies (Zimmennann and Potter 1982; Anfodillo et al. 2006; Lintunen and Kalliokoski 2010; Lee 2011; Schuldt et al. 2013). The study showed that VD and VF depend on the position along the flow PL as was demonstrated for tropical rainforest tree species (Schuldt et al. 2013). The role of PL could not be ignored (Becker et al. 2000; Anfodillo et al. 2006), as confirmed in this study. The VD decreased linearly, while the VF increased nonlinearly from the root to the branch. The PL explained 59.3 and 67.3 % of the longitudinal

Table 5 Regression analysis of hydraulically weighted average vessel diameters (VD, μm), vessel frequency (VF, mm^{-2}), theoretical specific hydraulic conductivity (k_s, kg m^{-1} MPa^{-1} s^{-1}) and theoretical vessel implosion resistance (VIR) against cambial age (CA, a) for the different parts of trees using the model $y = a + b\ln(x + c)$

Parts	a	b	c	R^2
Root				
VD	131.334	−0.457	0.011	0.309
VF	21.153	−0.172	−1	0.237
k_s	321.718	−4.010	0.062	0.429
VIR	−0.008	0.005	47.787	0.509
Stump				
VD	92.014	12.657	−0.496	0.876
VF	25.337	−2.057	−0.874	0.911
k_s	136.748	31.356	−0.381	0.745
VIR	0.018	−0.02	−0.976	0.693
Breast				
VD	70.095	21.190	−0.095	0.944
VF	30.547	−3.207	−0.749	0.911
k_s	69.553	69.511	0.286	0.813
VIR	0.020	0.002	0.063	0.761
Crown base				
VD	30.342	29.322	2.939	0.983
VF	36.153	−3.388	−0.598	0.969
k_s	−256.224	170.934	−7.509	0.968
VIR	0.024	0.002	−0.026	0.745
I Order branch				
VD	42.050	16.968	−0.587	0.957
VF	57.307	−6.439	−0.761	0.861
k_s	−651.880	233.046	24.989	0.940
VIR	0.039	−0.005	0.688	0.885
II Order branch				
VD	51.730	6.535	−0.675	0.969
VF	63.386	−3.450	−0.973	0.890
k_s	72.893	31.367	−0.096	0.958
VIR	0.028	−0.001	−0.982	0.770
III Order branch				
VD	32.066	10.947	1.443	0.988
VF	78.466	−6.266	−0.570	0.928
k_s	−39.980	59.894	5.459	0.965
VIR	0.042	−0.006	0.180	0.985

For VD and k_s in root, the model $y = a + bx + cx^2$ was used. Symbols a, b, c, and d are parameters of the model

R^2 is the percentage of variation explained by the model

The models are all significant at $P < 0.001$

variation in VD and VF of *B. platyphylla* trees (Fig. 2a, b). Vessels were the largest in the roots and tapered to the stems and further to the branches. This change is commonly referred to as vessel tapering (West et al. 1999; Anfodillo et al. 2006). Vessel tapering along the flow path likely helps the tree achieve an optimal structure for vascular element functioning (Tyree and Zimmermann 2002), maximize hydraulic conductivity and minimize xylem vulnerability.

One reason for vessel tapering is thought to be the control of water distribution as reported by researchers (Zimmermann 1978; Sellin et al. 2008). With the lowest conductivities at the end of the flow path (minor branches or petiole), the tree could control the distribution of water

and result in similar total conductance values from root to minor branch despite different PL. The other more reasonable reason is the control of auxin concentration (Aloni and Zimmermann 1983). Auxin is mainly secreted from developing buds and young shoots (Uggla et al. 1998; Scarpella and Meijer 2004), moves in a polar fashion through the vascular cambium (Sundberg et al. 2000; Aloni 2001). The basipetal polar flow of auxin from leaves to roots results in a gradient of decreasing auxin concentration from the apex to the stem base (Aloni and Zimmermann 1983; Lovisolo et al. 2002). Auxin regulates cambial activity to develop the secondary xylem (Nilsson et al. 2008). High concentrations cause cell fast differentiation, resulting in small and numerous vessels (Anfodillo et al.

2012). Low concentrations cause slow differentiation, resulting in large and few vessels. The decreasing auxin concentration results in a general increase in VD and decrease in VF from the branches to the stems and further to the roots.

Effects of cambial age

Above ground, VD increased in the first 10–20 years approximately from the pith and remained constant afterward (Fig. 3b, c). The pattern is consistent with the results by Guo et al. (2000), who studied radial variation of VD based on breast height of *Betula platyphylla*. The radial changes associated with cambial maturation (e.g., production of juvenile vs. mature wood) (Helińska-Raczkowska 1994). Vessel dimension is decided by initial cambial dimension. With age, the cambium becomes more and more mature, resulting in a change in the dimensions of cambial initials over time, which in turn affects the vessel dimension produced by the cambium (Plomion et al. 2001). The CA can fully explain radial variation in xylem structure, which has been confirmed in many studies (Helińska-Raczkowska 1994; Rao et al. 2002; Shi et al. 2008). In this study, the CA explained 87.6–98.8 % of the radial variation in VD and 86.1–96.9 % of that in VF above ground depending on the compartment (Table 5).

Interaction between PL and CA

Linear mixed-model analysis of variance showed that the effect of the interaction between PL and CA on vessel characteristics were significant (Table 3). For VD and VF, there were differences in the radial change rate with PL. The average radial change rate of VD and VF increased with PL. One plausible explanation for the variation of radial change rate with PL would be the effect of maturation of the apical meristems (Olesen 1978). There is strong evidence of this effect on cambial activity (Rossi et al. 2008). CA gradually decreased with increasing PL (Peterson et al. 2007). As a result, small cells were produced at the end of the flow pathway because of little CA (or immature cambium) (Bhat 1980) and higher auxin concentration (Anfodillo et al. 2012).

Notably, the differences in vessel characteristics were seen between the above ground and below ground parts of the trees. Vessels in the roots had larger VD and lower VF than those in the stem and branch locations. Larger vessels in roots were present to adapt water conductance along the path (West et al. 1999; Anfodillo et al. 2006; Lintunen and Kalliokoski 2010; Schuldt et al. 2013). Vessel characteristics between roots and
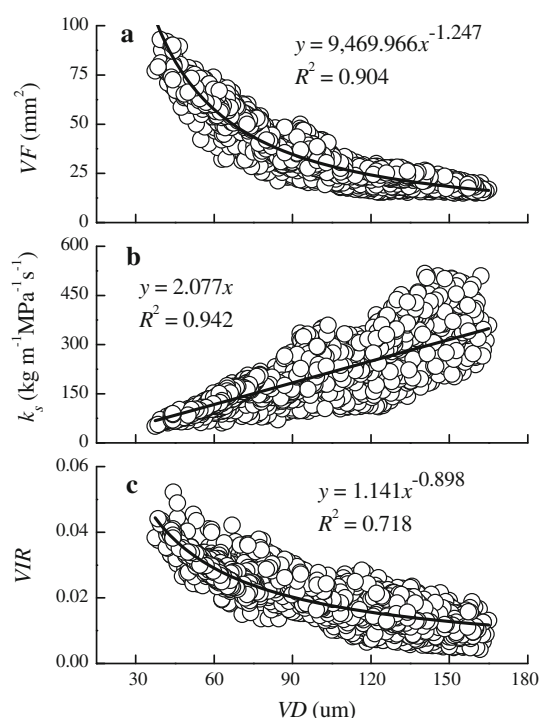

Fig. 4 Variations in vessel frequency (*VF*, mm^{-2}), theoretical specific hydraulic conductivity (k_s, kg m^{-1} MPa^{-1} s^{-1}), and theoretical vessel implosion resistance (*VIR*) with hydraulically weighted average vessel diameters (*VD*, μm) of the sampled trees. Based on all of the collected data, the *curves* were fitted by nonlinear or linear regression functions shown in the figure

stems (or branches) have been investigated in earlier studies (McElrone et al. 2004; Anfodillo et al. 2006; Pratt et al. 2007; Lintunen and Kalliokoski 2010; Lee 2011; Schuldt et al. 2013). However, fewer studies have examined the radial changes in vessel characteristics within roots (Vercambre et al. 2002; Christensen-Dalsgaard et al. 2008; Lintunen and Kalliokoski 2010). In the roots of *B. platyphylla*, VD and VF appeared to be constant with CA (Fig. 3a, d). The CA explained <51 % of the variation in the vessel characteristics within roots (Table 5). This showed that, in addition to CA, other factors caused the different change trends in the roots. First, the growing environments were different (Timell 1986; Schweingruber 2006). For example, the woody portion of the root is restrained by the soil. Drought adaptation may result in trees with stronger tissue and small vessels (Christensen-Dalsgaard et al. 2008). Second, the functions differed. In addition to water transport, roots also contribute to nutrient uptake, storage, and anchorage (Weiner and Thomas 2001) and are highly mechanically loaded throughout development (Fayle 1968; Christensen-Dalsgaard et al. 2008). As such, the vessels in the roots are responsible for all of

the functions as well as the growing environment, leading to a potential trade-off between them.

Hydraulic properties

The effects of PL and CA as well as their interaction on k_s are significant (Table 3). Futhermore, the change patterns of k_s with CA (or PL) were similar to that of VD (Figs. 2, 3). Conductivity decreased with vessel tapering (Fig. 4b). Similar findings were reported in other species (Spicer and Gartner 2001; Reyes-Santamaría et al. 2002; Sperry et al. 2006). When vessel tapering occurs, the VF increased nonlinearly (Fig. 4a). These findings were in accordance with studies of *Eucalyptus globulus* and *Eucalyptus nitens* (Hudson et al. 1998; Reyes-Santamaría et al. 2002) as well as *Persea americana* (Hudson et al. 1998; Reyes-Santamaría et al. 2002). Increased VF compensated for the partial loss of water volume caused by vessel tapering (McCulloh et al. 2003). A higher VF may minimize loss of hydraulic conductivity in cases in which part of the tissue is deactivated because of drought, freezing, or other injuries (West et al. 2000; De Micco et al. 2008). Vessels cannot shrink indefinitely, and here they eventually closed to a threshold of approximately 40 μm for VD in III order branch of *B. platyphylla*. VD in petiole or vein would be smaller.

Minimum vessel tapering values were confirmed using the West, Brown, and Enquist model (West et al. 1999). With the value of VD constant at the end of the flow path, a growing tree must adjust itself (e.g., reducing the auxin concentration to reduce the speed of cambium cell differentiation) to progressively increase the dimensions of the vessels at the stem base to maintain an optimized vascular network (West et al. 1999). Therefore, the VD is the largest in the stumps closest to the bark. However, the VD does not increase infinitely since a large VD is at greater risk of vulnerability to cavitation (Tyree and Sperry 1989; Sperry et al. 2006). Like k_s, VIR was affected significantly by PL, CA, and their interaction but showed the opposite change trend. The VIR decreased nolinearly with VD increasing (Fig. 4c). Clearly, the results supports the claim that large vessel may increace the hydraulic conductivity of the xylem but confer little resistance to cavitation (Tyree and Sperry 1989). The results suggest that a potential trade-off exists between conducting efficiency and safety (McElrone et al. 2004).

The theoretical values k_s and VIR were calculated according to the vessel characteristics in the current study. In fact, factors other than vessel sizes and quantities, such as vessel diameter histogram (Steppe and Lemeur 2007) or pit-field resistance (Hacke et al. 2006), affect k_s and VIR. To verify the calculated theoretical values, practical conducting efficiency and safety data also need to be detected for B. *platyphylla* trees in the future.

Conclusions

It is clear that the spatial change patterns of vessel characteristics in the secondary xylem of *B. platyphylla* depend on flow path-length and cambial age in the tree. The anatomical differences of the vessels in the secondary xylem within *B. platyphylla* suggest that the stumps close to the bark show lower vessel frequency, wider vessel diameters, more specific hydraulic conductivity, and higher vulnerability. However, the spatial patterns of xylem anatomy are complex and could not be easily attributed to one or two factors. Future studies should consider the effects of external and environmental factors to annual wood formation as well.

References

Aloni R (1987) Differentiation of vascular tissues. Annu Rev Plant Physiol 38:179–204

Aloni R (2001) Foliar and axial aspects of vascular differentiation: hypotheses and evidence. J Plant Growth Regul 20:22–34

Aloni R (2013) Role of hormones in controlling vascular differentiation and the mechanism of lateral root initiation. Planta 238:819–830

Aloni R, Zimmermann MH (1983) The control of vessel size and density along the plant axis: a new hypothesis. Differentiation 24:203–208

Anfodillo T, Carraro V, Carrer M, Fior C, Rossi S (2006) Convergent tapering of xylem conduits in different woody species. New Phytol 169:279–290

Anfodillo T, Deslauriers A, Menardi R, Tedoldi L, Petit G, Rossi S (2012) Widening of xylem conduits in a conifer tree depends on the longer time of cell expansion downwards along the stem. J Exp Bot 63:837–845

Becker P, Gribben RJ, Lim CM (2000) Tapered conduits can buffer hydraulic conductance from path-length effects. Tree Physiol 20:965–967

Bhat KM (1980) Variation in structure and selected properties of Finnish birch wood. I Interrelationships of some structural features, basic density and shrinkage. Silva Fenn 14:384–396

Bhat KM, Karkkainen M (1981) Variation in structure and selected properties of Finnish birch wood: IV. Fibre and vessel length in branches, stems and roots. Silva Fenn 15:10–17

Christensen-Dalsgaard KK, Ennos AR, Fournier M (2008) Are radial changes in vascular anatomy mechanically induced or an ageing process? Evidence from observations on buttressed tree root systems. Trees 22:543–550

Czkowski SZ (1973) Auxin stimulation of cambial activity in *Pinus silvestris* I. The differential cambial response. Physiol Plant 29:281–287

De Micco V, Aronne G, Baas P (2008) Wood anatomy and hydraulic architecture of stems and twigs of some Mediterranean trees and shrubs along a mesic-xeric gradient. Trees 22:643–655

Fan ZX, Cao KF, Becker P (2009) Axial and radial variations in xylem anatomy of angiosperm and conifer trees in Yunnan, China. Iawa J 30:1–13

Fayle DCF (1968) Radial growth in tree roots: distribution, timing, anatomy. Faculty of Forestry, University of Toronto, Toronto

Gartner BL (1995) Hydraulic and mechanical consequences. Academic, San Diego, p 125

Goldstein H (2011) Multilevel statistical models, vol 922. Wiley, New York

Guo MH, Pan YJ, Chen GS (2000) The radial variation patterns of anatomical characteristics of *Betula platyphylla* wood in dfiierent altitude. J Northwest For Univ 28:25–29

Hacke UG, Sperry JS (2001) Functional and ecological xylem anatomy. Perspect Plant Ecol Evol Syst 4:97–115

Hacke UG, Sperry JS, Pockman WT, Davis SD, McCulloh KA (2001) Trends in wood density and structure are linked to prevention of xylem implosion by negative pressure. Oecologia 126:457–461

Hacke UG, Sperry JS, Wheeler JK, Castro L (2006) Scaling of angiosperm xylem xtructure with safety and efficiency. Tree Physiol 26:689–701

He CX, Li JY, Guo M (2007) Research progresses of the mechanism of the sap flow in trees. Acta Ecol Sin 27:329–337

Helińska-Raczkowska L (1994) Variation of vessel lumen diameter in radial direction as an indication of the juvenile wood growth in oak (*Quercus petraea* Liebl). Ann For Sci 51:283–290

Hudson I, Wilson L, Van Beveren K (1998) Vessel and fibre property variation in *Eucalyptus globulus* and *Eucalyptus nitens*: some preliminary results. Iawa J 19:111–130

Jacobsen A, Agenbag L, Esler KJ, Partt RB, Ewers FW, Davis SD (2007) Xylem density, biomechanics and anatomical traits correlate with water stress in 17 evergreen shrub species of the Mediterranean-type climate region of South Africa. J Ecol 95:13

James SA, Meinzer FC, Goldstein G, Woodruff D, Jones T, Restom T, Mejia M, Clearwater M, Campanello P (2003) Axial and radial water transport and internal water storage in tropical forest canopy trees. Oecologia 134:37–45

Kalliokoski T, Nygren P, Sievanen R (2008) Coarse root architecture of three boreal tree species growing in mixed stands. Silva Fenn 42:189–210

Lachenbruch B, Moore JR, Evans R (2011) Radial variation in wood structure and function in woody plants, and hypotheses for its occurrence. In size-and age-related changes in tree structure and function, vol 4. Springer, Heidelberg, pp 121–164

Lee MR (2011) Comparison of quantitative vessel element and wood fiber features between stem and root wood of yellow-poplar (*Liriodendron tulipifera* L.). 한국목재공학술발표논문집 2011, pp 6–7

Leitch MA (2001) Vessel-element dimensions and frequency within the most current growth increment along the length of *Eucalyptus globulus* stems. Trees 15:353–357

Lin JX (1993) Notes on the improvements of wood-sectioning techniques. Chin Bull Bot 10:61–64

Lintunen A, Kalliokoski T (2010) The effect of tree architecture on conduit diameter and frequency from small distal roots to branch tips in *Betula pendula*, *Picea abies* and *Pinus sylvestris*. Tree Physiol 30:1433–1447

Lovisolo C, Schubert A, Sorce C (2002) Are xylem radial development and hydraulic conductivity in downwardly-growing grapevine shoots influenced by perturbed auxin metabolism? New Phytol 156:65–74

Martínez-Cabrera HI, Jones CS, Espino S, Schenk HJ (2009) Wood anatomy and wood density in shrubs: responses to varying aridity along transcontinental transects. Am J Bot 96:1388–1398

McCulloh KA, Sperry JS, Adler FR (2003) Water transport in plants obeys Murray's law. Nature 421:939–942

McElrone AJ, Pockman WT, Martínez-Vilalta J, Jackson RB (2004) Variation in xylem structure and function in stems and roots of trees to 20 m depth. New Phytol 163:507–517

Nilsson J, Karlberg A, Antti H, Lopez-Vernaza M, Mellerowicz E, Perrot-Rechenmann C, Sandberg G, Bhalerao RP (2008) Dissecting the molecular basis of the regulation of wood formation by auxin in hybrid aspen. Plant Cell 20:843–855

Olesen PO (1978) On cyclophysis and topophysis. Silvae Genet 27:173–178

Olson ME, Rosell JA (2013) Vessel diameter-stem diameter scaling across woody angiosperms and the ecological causes of xylem vessel diameter variation. New Phytol 197:1204–1213

Peterson MG, Dietterich HR, Lachenbruch B (2007) Do Douglas-fir branches and roots have juvenile wood? Wood Fiber Sci 39:651–660

Petit G, Anfodillo T, Mencuccini M (2007) Tapering of xylem conduits and hydraulic limitations in sycamore (*Acer pseudoplatanus*) trees. New Phytol 177:653–664

Plomion C, Leprovost G, Stokes A (2001) Wood formation in trees. Plant Physiol 127:1513–1523

Pratt RB, Jacobsen AL, Ewers FW, Davis SD (2007) Relationships among xylem transport, biomechanics and storage in stems and roots of nine Rhamnaceae species of the California chaparral. New Phytol 174:787–798

Rao RV, Shashikala S, Sreevani P, Kothiyal V, Sarma CR, Lal P (2002) Within tree variation in anatomical properties of some clones of *Eucalyptus tereticornis* Sm. Wood Sci Technol 36:271–285

Reyes-Santamaría I, Terrazas T, Barrientos-Priego AF, Trejo C (2002) Xylem conductivity and vulnerability in cultivars and races of avocado. Sci Hortic (Amsterdam) 92:97–105

Rossi S, Deslauriers A, Anfodillo T, Carrer M (2008) Age-dependent xylogenesis in timberline conifers. New Phytol 177:199–208

Scarpella E, Meijer AH (2004) Pattern formation in the vascular system of monocot and dicot plant species. New Phytol 164:209–242

Schuldt B, Leuschner C, Brock N, Horna V (2013) Changes in wood density, wood anatomy and hydraulic properties of the xylem along the root-to-shoot flow path in tropical rainforest trees. Tree Physiol 33:161–174

Schulte PJ (2012) Vertical and radial profiles in tracheid characteristics along the trunk of Douglas-fir trees with implications for water transport. Trees 26:421–433

Schweingruber FH (2006) Anatomical characteristics and ecological trends in the xylem and phloem of Brassicaceae and Resedaceae. Iawa J 27:419

Sellin A, Rohejärv A, Rahi M (2008) Distribution of vessel size, vessel density and xylem conducting efficiency within a crown of silver birch (*Betula pendula*). Trees 22:205–216

Shi L, Sun QF, Deng J (2008) Study on anatomical structure variation and chemical properties of Introduced *Dalbergia sissoo* Roxb. For Res 21:212–216

Sperry JS, Hacke UG, Pittermann J (2006) Size and function in conifer tracheids and angiosperm vessels. Am J Bot 93:1490–1500

Spicer R, Gartner BL (2001) The effects of cambial age and position within the stem on specific conductivity in Douglas-fir (*Pseudotsuga menziesii*) sapwood. Trees 15:222–229

Steppe K, Lemeur R (2007) Effects or ring-porous and diffuse-porous stem wood anatomy on the hydraulic parameters used in water flow and storage model. Tree Physiol 27:43–52

Sundberg B, Uggla C, Tuominen H (2000) Cambial growth and auxin gradients. In: Savidge RA, Barnett JR, Napier R (eds) Cell and molecular biology of wood formation. Experimental biology reviews. BIOS, Oxford, pp 169–188

Timell TE (1986) Compression wood in Gymnosperms. vol 3. Ecology of compression wood formation, silviculture and compression wood, mechanism of compression wood action, compression wood in the lumber and pulp and paper industries, compression wood induced by the balsam woolly aphid, opposite wood. Springer, New York

Tyree MT, Sperry JS (1989) Vulnerability of xylem to cavitation and embolism. Annu Rev Plant Biol 40:19–36

Tyree MT, Zimmermann MH (2002) Xylem structure and the ascent of sap, 2nd edn. Springer, Berlin

Uggla C, Mellerowicz EJ, Sundberg B (1998) Indole-3-acetic acid controls cambial growth in Scots pine by positional signaling. Plant Physiol 117:113–121

Vercambre G, Doussan C, Pages L, Habib R, Pierret A (2002) Influence of xylem development on axial hydraulic conductance within *Prunus* root systems. Trees 16:479–487

Wang C (2006) Biomass allometric equations for 10 co-occurring tree species in Chinese temperate forests. For Ecol Manag 222:9–16

Weiner J, Thomas SC (2001) The nature of tree growth and the "age-related decline in forest productivity". Oikos 94:374–376

West GB, Brown JH, Enquist BJ (1999) A general model for the structure, function, and allometry of plant vascular systems. Nature 400:664–667

West GB, Brown JH, Enquist BJ (2000) The origin of universal scaling laws in biology. Scaling Biol 263:87–112

Yu HP, Liu YX, Zhi CY, Liu ZB (2008) Measurement of wood microstructural parameters on transverse section by binary morphology. Mater Sci Technol 16:107–111

Zach A, Schuldt B, Brix S, Horna V, Culmsee H, Leuschner C (2010) Vessel diameter and xylem hydraulic conductivity increase with tree height in tropical rainforest trees in Sulawesi, Indonesia. Flora Morphol Distrib Funct Ecol Plants 205:506–512

Zimmermann MH (1978) Hydraulic architecture of some diffuse-porous trees. Can J Bot 56:2286–2295

Zimmennann MH, Potter D (1982) Vessel-length distribution in branches, stem and roots of *Acer rubrum* L. IAWA Bull (NS) 3:103–109

Zobel BJ, Buijtenen JPv (1989) Wood variation: its causes and control. Springer, Berlin